

Article

Turbidite Fan Deposits in Gentle Slope Zones of Continental Faulted Basins: A Case Study from the Chezhen Depression, Bohai Bay Basin

Junyang Cheng ¹, Xianke He ¹, Dongping Duan ¹ and Jingzhe Li ^{2,3,*}¹ Shanghai Branch of CNOOC Ltd., Shanghai 200335, China; chengjy4@cnooc.com.cn (J.C.)² State Key Laboratory of Oil and Gas Reservoir Geology and Exploitation, Chengdu University of Technology, Chengdu 610059, China³ College of Electromechanics, Qingdao University of Science and Technology, Qingdao 266061, China

* Correspondence: lijingzhe@qust.edu.cn

Abstract: Turbidite fans, serving as good reservoirs for petroleum accumulation, are typically formed during deep faulting periods in continental basins, particularly in steep slope zones. However, gentle slope zones are also significant and unique for the formation of turbidite fans. These turbidite fans hold immense importance in exploring concealed lithological reservoirs. Taking the Chezhen Depression of Bohai Bay Basin as an example, we conducted a comprehensive study of the turbidite fan deposits in the gentle slope zone. Our results indicate that (1) small-scale distal-source turbidite fans are a common sedimentary type in the Chezhen Depression of the Bohai Bay Basin; (2) the study area is mainly characterized by seven lithofacies; (3) there are incomplete Bouma sequences in the study interval. This study is an important turbidite investigation into continental faulted basins, and it can also provide an important reference value for exploration and development in unconventional reservoirs of the same type.

Keywords: gentle slope zone; continental faulted basin; Chezhen Depression; turbidite fan; sedimentary characteristics



Citation: Cheng, J.; He, X.; Duan, D.; Li, J. Turbidite Fan Deposits in Gentle Slope Zones of Continental Faulted Basins: A Case Study from the Chezhen Depression, Bohai Bay Basin. *Processes* **2023**, *11*, 2001. <https://doi.org/10.3390/pr11072001>

Academic Editors: Jianhua Zhao, Guoheng Liu, Xiaolong Sun and Yuqi Wu

Received: 30 May 2023

Revised: 24 June 2023

Accepted: 27 June 2023

Published: 3 July 2023



Copyright: © 2023 by the authors. Licensee MDPI, Basel, Switzerland. This article is an open access article distributed under the terms and conditions of the Creative Commons Attribution (CC BY) license (<https://creativecommons.org/licenses/by/4.0/>).

1. Introduction

The study of turbidite fan reservoirs has become an increasingly popular research topic due to its significance as an important lithologic reservoir. Turbidite fans are diverse and can be classified into various types, such as submarine fans, lacustrine fans, nearshore subaqueous fans, and slump turbidite fans, all of which are mainly formed by turbidity currents. Since the middle of the last century, the study of turbidity currents and their sedimentary products has been highly valued by researchers. For example, Bouma systematically summarized the characteristics of the vertical sequence of turbidite deposits and put forward the Bouma sequence [1–3]. Later, some studies combined modern sedimentation with laboratory experiments and seismic data to gain insights into the internal geometry of turbidite lobes, leading to the establishment of classical facies models [4–8]. With the advancement of analytical testing and computer simulation methods, the triggering and movement mechanisms of turbidity currents, as well as their interaction with other geological conditions, have been extensively studied. Additionally, the theories of the genesis, classification, and internal properties of turbidite reservoirs have been continuously updated and refined [9–15].

In continental faulted basins in eastern China, turbidite fans formed during deep faulting periods provide many good reservoirs for oil and gas resources. Many researchers have put forward localized models and have made a lot of important achievements in our understanding. For the Jiyang Sub-basin, especially for its steep slope zone, many detailed models have been put forward, such as a fault-erosion type of steep slope model, an

intermittent type of steep slope model, and a continuous type of steep slope model [16]. As for plane distribution, the geophysical identification method, and the forming mechanism of reservoirs in steep slope zones, many other scholars have also made a lot of in-depth contributions [17,18].

Compared with those in steep slope zones, turbidite fans developed in gentle slope zones are also very important and unique [19]. However, previous studies mostly focused on steep slope zones or depression zones, and focused less on gentle slope zones.

In this paper, we introduced a kind of small-scale turbidite fan developed in the gentle slope zone of a continental fault basin. A case from the third member of the Shahejie Formation in the Chezhen Depression was used as an example to analyze its internal structure and explore its spatial distribution rules. The results of this paper are expected to provide some theoretical support for the hydrocarbon exploration and development of such types of reservoirs.

2. Geological Settings

The Chezhen Depression is a dustpan-shaped sag, with steep slopes to the north and gentle slopes to the south. The northern steep slope zone is attached to the south side of the Chengzikou Uplift, while the southern gentle slope zone is adjacent to the north slope of the Wudi Uplift and Yihezhuang Uplift. Within the southern gentle slope zone, a group of NE-trending arc-shaped faults have developed, forming the Caozhuang fault zone. The study area is located at the transition between the fault zone and the center of the sag (Figure 1). Based on sedimentological studies, the provenance of the sediment in the study area can be traced back to the Wudi and Yihezhuang Uplifts, indicating a distant sediment source [20,21].

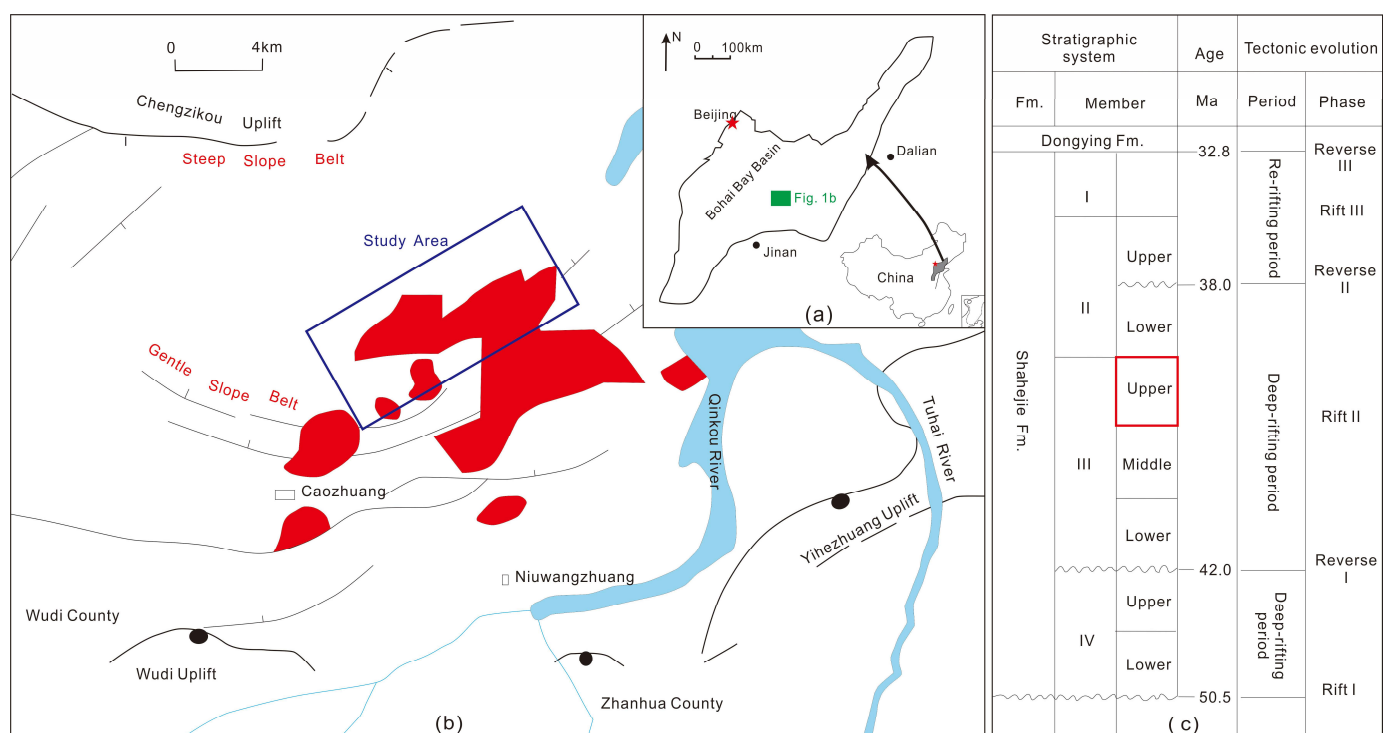


Figure 1. (a) Location map of the Bohai Bay Basin highlighting the Chezhen Depression. (b) Structural map of the Chezhen Depression (purple box: the study area; the red areas: areas rich in oil and gas reserves). (c) Generalized stratigraphy of the Shahejie Formation in the study area (red box: the target interval) (modified from [22,23]).

The study area primarily consists of Cenozoic strata, including the Paleogene Shahejie Formation and Dongying Formation, as well as the Neogene Guantao Formation,

Minghuazhen Formation, and Quaternary Pingyuan Formation, arranged from bottom to top. Within the study area, the third member of the Shahejie Formation (Es3) is a significant hydrocarbon-bearing interval. According to lithologic associations, the Es3 can be subdivided into three sub-members, from bottom to top: Es3L, Es3M, and Es3U. The lower part of Es3L mainly comprises sandy mudstone mixed with conglomeratic sandstone and biological limestone, while the remaining Es3L and Es3M primarily consist of brown oil shale and oil shale. Es3U is mainly composed of gray and grayish-brown mudstone with siltstone and fine sandstone. Among these three sub-members, Es3U is the most important target section for hydrocarbon exploration and development [24–28].

Based on climate analysis, the sedimentation period of the Es3U in the study area was characterized by a humid climate with sufficient rainfall and forest-dominated vegetation. The sedimentation during this period was a typical lake regression deposit resulting from a lake-level drop. From the perspective of tectonic evolution, the sedimentation during the Es3U period occurred during the mid to late stage (deep faulting period) of the lake basin's rifting phase. Overall, this sedimentary environment was a semi-deep lake to deep lake depositional environment [29].

3. Materials and Methods

This study primarily utilized well logging data from 234 drilling wells with a mean horizontal distance of approximately 300 m. Additionally, 13 of these wells contained core samples totaling 547.3 m in length. Based on these core samples, many photographs were taken, and rock and mineral identification as well as physical property analysis were also conducted.

In this study, we established an isochronous stratigraphic framework for the Es3U interval in the study area. To achieve this, we adopted a “cyclic comparison and hierarchical control” stratigraphic comparison method. We used stable shale marker beds as a reference to establish the framework, which are characterized by distinct lithological and electrical properties and exhibit relatively consistent distributions with good isochronous characteristics. By using these marker beds as a control, we made stratigraphic divisions and comparisons based on seismic characteristics and logging cycle variations. Within this isochronous stratigraphic framework, we analyzed lithology and sedimentary structure characteristics based on core and well-logging data and classified the lithofacies according to their characteristics. We then combined these lithofacies with wire-line log curves to identify the log facies types. Next, we analyzed the sedimentary sequences of individual wells and examined the distribution characteristics of sand bodies between multiple wells. Based on these results, we analyzed the sedimentary environment of the turbidite fan, discussed the sedimentary microfacies and lithofacies characteristics, and then analyzed the lateral migration and evolution characteristics of the fan body. We conducted a case study of the migration and evolution of a turbidite fan body. Finally, on the basis of a detailed dissection of the internal structure of the turbidite fan body, we established a sedimentary model for the turbidite fan deposits.

4. Results

4.1. Lithology and Sedimentary Structures

The most notable lithological feature of the Es3U sub-section of the Es3 member is “sandstone enveloped by mudstone”, with the mudstone primarily exhibiting gray and black colors. The sandstone is mostly gray or gray-white in color, composed mainly of lithic–feldspathic fine sandstone with sub-angular grains. Its sorting characteristics are typically moderate to well sorted, mainly supported by grain-to-grain contact and point-line contact, with the development of pore-type and pore-contact cementation (Table 1). Quartz content ranges from 40 to 50%, feldspar accounts for approximately 30–40%, and lithic fragments comprise 15–25% of the composition. Overall, the sandstone exhibits relatively high feldspar and lithic content, as well as low sandstone maturity.

The sedimentary structures in the Es3U sub-section of the Sha-3 formation are diverse. By studying the core samples from 13 wells in the area, sedimentary structures such as pillow structures, load-flame structures, slump structures, pressure-solution structures, convolute bedding, mud–gravel transition structures, and mudstone tearing debris can be observed (Figure 2).



Figure 2. Common sedimentary structures in the study area. ((a). Sand pillow, X408 well, 2649 m; (b). sour face, X40 well, 2642 m; (c). heavy-charge/flame, X408 well, 2650.1 m; (d). slump, X441 well, 2618.5 m; (e). convolute bedding, X441 well, 2663.8 m; (f). ripped mudstone clast, X408 well, 2643.8 m; (g). wavy bedding, X142 well, 2874.3 m; (h). massive structure in mudstone, X40 well, 2629.7 m; (i). biogenic traces in shaly-sand, X40 well, 3153.5 m).

4.2. Lithofacies

Based on the sedimentary structure, bedding, and lithology characteristics, and with reference to previous studies, this research divided the facies of the turbidite fan in the study area into two categories, sandstone facies and mudstone facies, which were further subdivided into seven types, including conglomeratic sandstone facies, parallel-bedded fine sandstone facies, and interbedded fine sandstone facies (Table 2).

Table 1. Petrographic analysis of the X40 well.

Well	Depth (m)	Particle Composition (%)			Filling Material(%)			Contact Relation	Cement Type	Contact Relation	Sorting	Roundness
		Quartz	Feldspar	Rock Fragments	Cementation		Matrix					
					Calcite	Dolomite	Mud					
X40	2640.5	45	31	24	9	1	4	Grain	Pore	Line-point	moderate	Sub-angular
	2644.3	48	36	16	5	2	5	Grain	Pore	Line-point	well	
	2648.4	50	30	20	10	/	3	Grain	Pore	Line-point	moderate	
	2652.1	48	36	16	7	1	6	Grain	Pore-contact	Line-point	moderate	
	2657.5	45	36	19	5	1	6	Grain	Pore-contact	Line-point	moderate	
	2660.5	45	36	19	2	4	6	Grain	Pore-contact	Line-point	moderate	

Table 2. Lithofacies classification of the turbidite fan in the study area.

	Lithofacies	Sedimentary Features
Sandstone facies	Sc: Conglomeratic sandstone facies	Finely to coarsely graded, with scour or distinct contact at the base, may contain mud clasts or gravels, massive bedding
	Sh: Parallel-bedded fine sandstone facies	Fine-grained, moderately well-sorted, with parallel bedding, less commonly developed
	Sr: Interbedded fine sandstone facies	Small-scale cross-bedding, ripple bedding, thin bedding, less commonly developed
	Sbm: Fine sandstone facies with Bouma sequences	Thin interbeds with alternation of parallel and lenticular laminae, interbedded with mudstones
	Sl: Fine sandstones with slump features	Interbeds of fine sandstones and mudstones, with typical soft-sediment deformation structures such as slumps and sand pillows developed
Mudstone facies	Fsm: Dark mudstone facies	Dark gray or black, blocky, sometimes with weak horizontal lamination
	Fl: Sandy mudstone facies	Mudstones interbedded with thin sandstone beds, with fine horizontal lamination or weak ripple lamination.

(1) Sandstone facies:

The sandstone facies in the study area include conglomeratic sandstone facies (Sc), parallel-bedded fine sandstone facies (Sh), interbedded fine sandstone facies (Sr), fine sandstone facies with Bouma sequences (Sbm), and slump facies (Sl).

Conglomeratic sandstone facies (Sc): This is an important rock type in the study area. It consists mainly of fine-grained sandstones or siltstones, with some layers containing pebbles or mud clasts. Different sizes of scour surfaces are developed, and sedimentary structures such as massive bedding or slight bedding are observed.

Parallel-bedded fine sandstone facies (Sh): This facies is generally fine-grained, mainly consisting of fine sandstones, and moderately well-sorted. Parallel bedding is commonly developed. However, this facies is not commonly observed in the study area.

Interbedded fine sandstone facies (Sr): This facies is mainly composed of fine sandstones and siltstones, with small-scale cross-bedding and ripple bedding developed. This facies is commonly associated with the parallel-bedded fine sandstone facies, but it is not commonly observed in the study area.

Fine sandstone facies with Bouma sequences (Sbm): This facies is a typical turbidite, characterized by thin interbeds of sandstone and mudstone. The rock type mainly consists of fine sandstones and siltstones, with typical gravity flow sedimentary structures such as sand pillows and flame structures (Figure 2c).

Slump facies (Sl): This facies mainly occurs in the interbeds of fine sandstones and mudstones, with typical soft-sediment deformation structures such as slumps and sand pillows developed (Figure 2d).

(2) Mudstone facies:

The mudstone facies mainly include dark mudstone facies (Fsm) and sandy mudstone facies (Fl) (Figure 3).

Dark mudstone facies (Fsm): The mudstone is mainly gray or dark gray in color, and massive in structure, sometimes with weak horizontal lamination.

Sandy mudstone facies (Fl): The rock type mainly consists of mudstones interbedded with thin sandstone beds, with fine horizontal lamination or weak ripple lamination developed.



Figure 3. Core photos of X408 well. (a): Overall photo of the core box; (b): a sample of Fsm; (c): a sample of Fl.

4.3. Log Facies Characteristics

Based on the analysis of lithology, sedimentary structures, and lithofacies characteristics, combined with logging response characteristics, seven log facies types (I~VII) were identified, and the lithology and electrical characteristics of each log facies type were summarized (Table 3). Among them, types I and III are dominated by sandstones, typically exhibiting a thickness greater than 4 m and representing the main sand body types. Types II, IV, V, and VI comprise both sandstones and mudstones, but the former is less abundant. Finally, type VII is primarily composed of mudstones.

4.4. Sedimentary Sequence Characteristics

Through detailed core description, we established a vertical sedimentary evolution sequence for Es3U in the study area. The sand bodies in the study area mainly exhibit regular rhythms, and the lithological distribution sequence from bottom to top generally comprises a combination of (muddy) fine-grained sandstone, siltstone, muddy siltstone, and mudstone. We also identified incomplete Bouma sequences in the study area, with visible ABC and BC sections in the channel sand bodies, and typical turbidite sedimentation between channels, commonly featuring CDE and DE sections (Figure 4).

4.5. Characteristics of Sand Body Distribution

The distribution of single-well turbidite fan bodies and inter-well comparisons indicate that in the study area, the thickness of single-stage turbidite sand bodies is generally less than 6 m, and they exhibit a “mud enveloping sand” characteristic in the vertical direction, with sandstone content generally not exceeding 20%. The distribution of turbidite fan bodies is unstable in the lateral direction, with each individual fan body exhibiting a relatively small spread range, generally not exceeding 1–2 well spacings, and the majority of fan body areas are smaller than 3 km², with an average of 1.7 km². According to statistics, the width of the main channel in the study area ranges from 90 to 760 m, with a large variation range, and most of them are distributed between 100 and 300 m, with an average width of around 260 m.

Table 3. Classification of log facies in the study area.

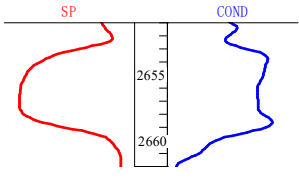
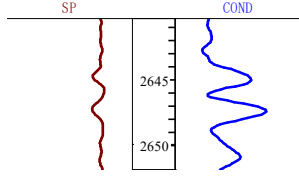
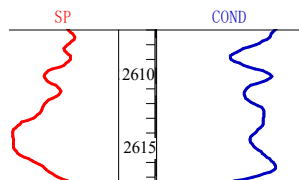
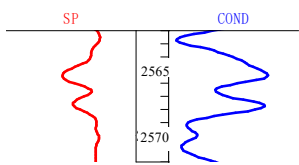
Facies	Subfacies	Microfacies	Lithological and Electrical Characteristics	Log Facies	
Turbidite fan	Inner fan	Main channel	Pebble-bearing sandstone is the main type, and the erosion surface is developed. The logging curve is bell-shaped or box-shaped, and the thickness of sandstone is generally >4~6 m.		Type I
	Middlefan	Main channel levee	The lithology is fine, and the SP curve is a low-amplitude straight or micro-toothed curve. The thickness of sandstone is generally less than 2~4 m.		Type II
		Braided channel	It is mainly composed of fine sandstone and silty fine sandstone. The ABC section of Bouma sequence is developed. The SP curve is box-shaped, bell-shaped and a combination type. The thickness of sandstone is generally >4 m.		Type III
		Between braided channels	The shaly sandstone and siltstone are mainly intercalated with thin layers of mud. The SP curve shows a tooth shape and finger shape with medium-low amplitude. The thickness of sandstone is generally <2~4 m.		Type IV

Table 3. Cont.

Facies	Subfacies	Microfacies	Lithological and Electrical Characteristics	Log Facies	
		The front of middle fan	It is mainly composed of thin fine-siltstone and mudstone interbeds. The natural potential curve is medium-low-amplitude finger shape, and the thickness of sandstone is generally less than 2 m.		Type V
		Lobe	It is dominated by silty fine sandstone, and the SP curve shows a medium-low funnel and funnel-box combination. The thickness of sandstone is generally >2–4 m.		Type VI
	Outer fan	Terminal	They are mainly muddy siltstone and dark mudstone. The SP curve is characterized by serrated and mudstone baseline with extremely low amplitude. The thickness of sandstone is generally less than 1 m.		Type VII

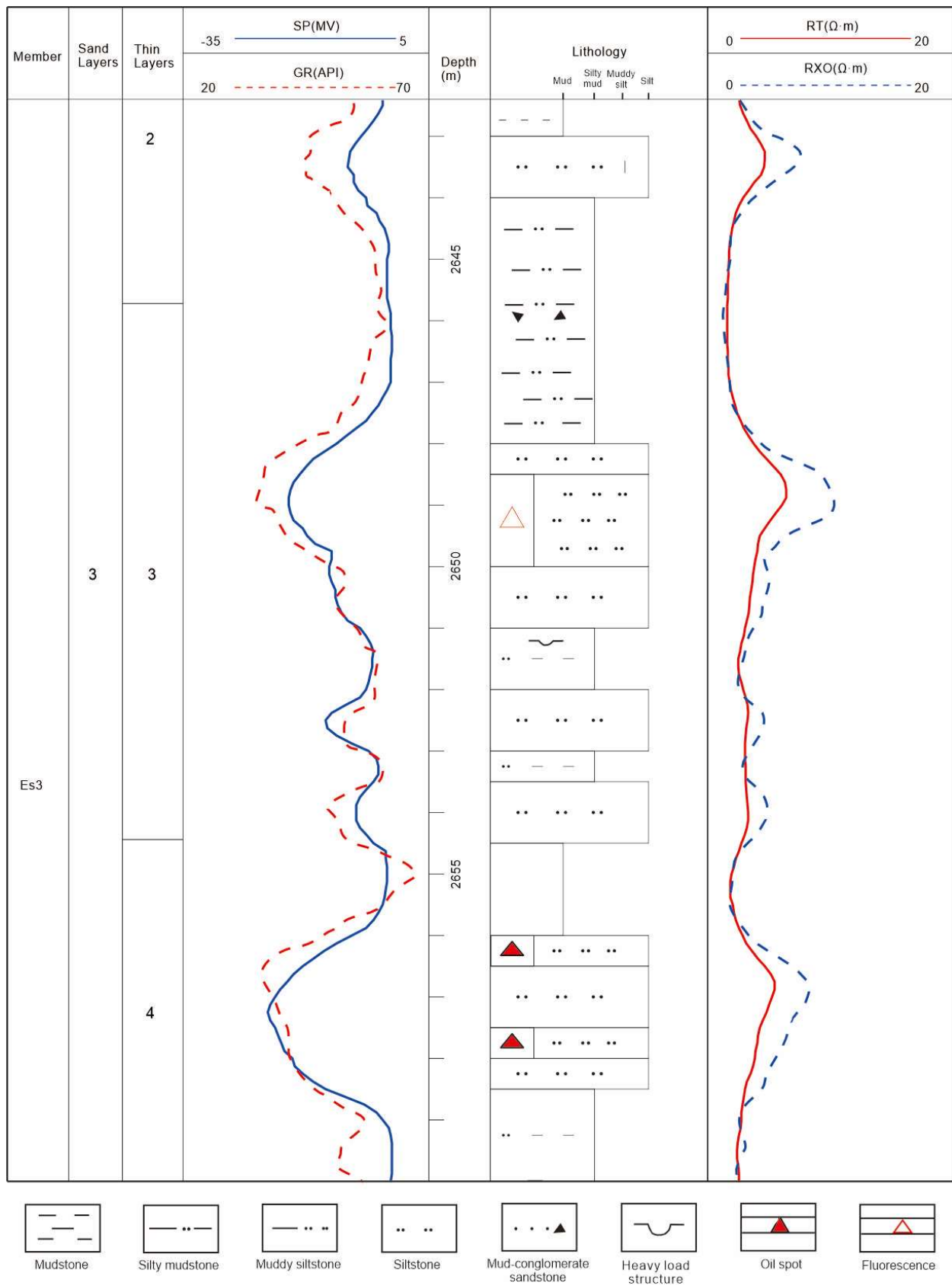


Figure 4. The vertical facies pattern of X408 well.

5. Discussions

5.1. Sedimentary Environments

The study area is located in the gentle slope zone of a continental rift basin. Sediments have been transported over long distances, generally resulting in finer lithology, with mainly fine sandstone and siltstone, and with some layers containing a small amount of mudstone. Mudstone is an important sedimentary environmental indicator that can reflect various information such as driving force, original topography, transport distance, and surrounding environment [13,30–34]. In particular, gray or black mudstone sediment represents a reducing environment [27,35–37]. Previous studies have shown that long transportation distances with a certain slope often lead to secondary transportation and/or a certain degree of sliding deformation, which favor the formation of diverse gravity flow sedimentary structures [15,38–42]. The study area precisely meets these favorable conditions, being situated in the center of the depression and characterized by the development of turbidite fan sedimentation.

The composition maturity and structural maturity of the sedimentary bodies of turbidite fans in the study area are low, which is closely related to the turbidite genesis of reservoirs, showing significant differences from deltaic or shoreface sand bodies in the gentle slope zone of a continental rift basin [43]. Similarly, if deltaic or shoreface sand bodies are deposited in the same zone, and the sand body is transformed repeatedly by waves, the structural maturity and composition maturity of the sandstone will be significantly higher.

5.2. Characteristics of Facies and Lithofacies

Based on the sedimentary characteristics of the fan bodies in the study area, turbidite fans can be divided into three sub-facies: inner fan, middle fan, and outer fan. The inner fan can be further divided into the main channel and the main channel margin microfacies, while the middle fan comprises braid-channel, inter-braid-channel, lobe, and fan body front microfacies (Table 3).

The middle fan sub-facies constitute the main body of turbidite fan sedimentation, and the braid-channel sedimentation determines the shape and size of the fan body, serving as the most important sand body type in turbidite fan sedimentation. Typically containing mud clasts and scour surfaces at the bottom, braid-channel sedimentation forms the framework of fan body sedimentation. The main channel and lobe sedimentation in the inner fan can also form good reservoirs, but their distribution range is relatively small. The main channel margin, inter-braid channel, fan body front, and outer fan are mainly composed of muddy or thinly layered siltstone sedimentation, resulting in poor reservoir properties, and thus, they are not the main reservoir types.

From the lithofacies analysis, conglomeratic sandstone facies (Sc), parallel laminated fine sandstone facies (Sh), and cross-laminated fine sandstone facies (Sr), which typically occur in the inner fan main channel or middle fan braided channel, are products of deposition under strong hydrodynamic conditions and generally form high-quality reservoirs [44,45]. On the other hand, fine-grained sandstone facies with Bouma sequences (Sbm), slumping facies (Sl), and other facies typically develop in the middle fan braided channel, fan front, and outer fan facies belts. The sediment grain size is finer than that of facies developing in the channels, and they can form some reservoirs, but the quality is significantly worse. Dark mudstone facies (Fsm) and sandy mudstone facies (Fl) often develop between the braided channels, which are the result of flood deposition and are generally non-reservoir facies.

5.3. Characteristics of Fan Body Migration

The planar migration of a turbidite fan is frequent, and the size of the fan changes continuously during different stages [7]. Taking the example of the three-stage fan developed in a certain interval, the migration and evolution process of the fan is explained. During the deposition of the first-stage fan, the size of the fan was relatively small. The main part of the fan was encountered in well X-18-19, and the edge of the fan was revealed in well X-21-19. The second-stage fan was developed on the basis of the first-stage fan, and the

size of the fan was slightly expanded. Due to the infilling effect of earlier sedimentation, the second-stage waterway sedimentation migrated slightly to the left. Well X-18-19 was still located in the main part of the fan, while the fan migrated to well X-17-17 on the left. The third-stage fan continued to increase in size on the basis of the second-stage fan, and it basically covered the first- and second-stage fans (Figure 5).

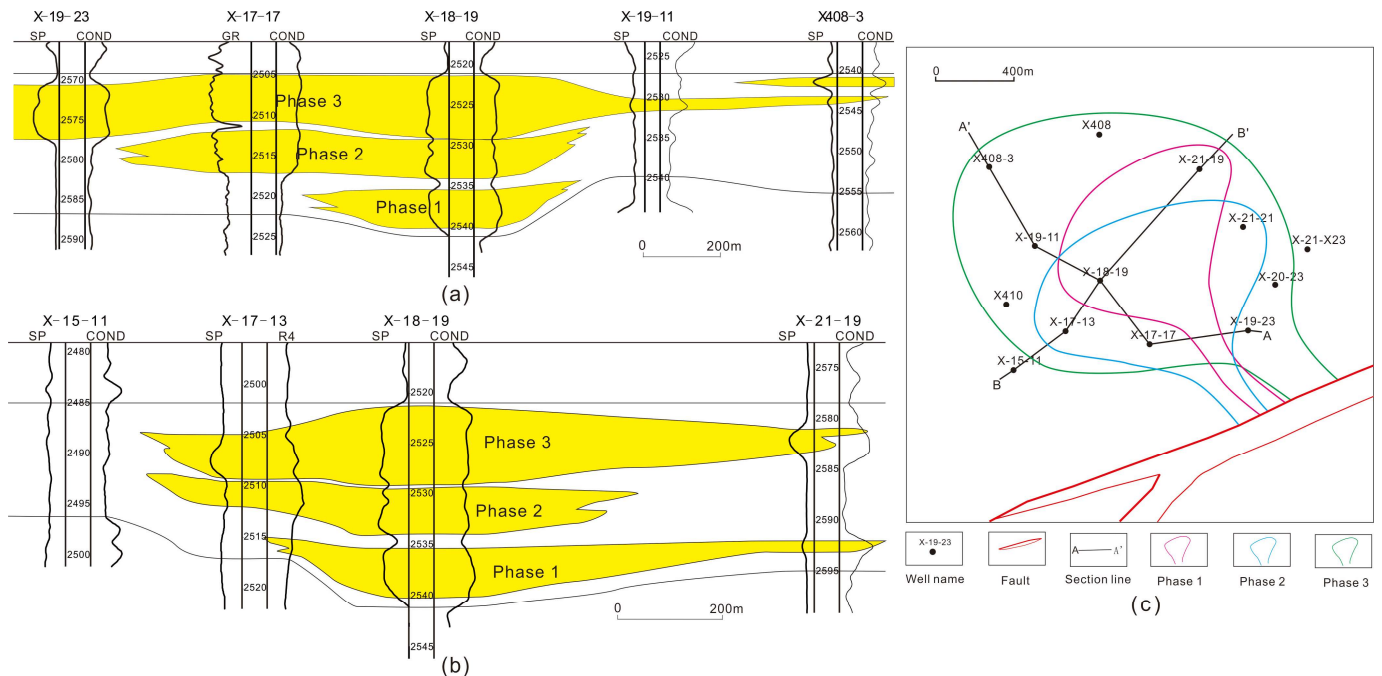


Figure 5. Schematics of a 3-phase fan migration evolution. (a) Longitudinal section comparison chart of 3 fan bodies (AA'); (b) cross-section comparison chart of 3 fan bodies (BB'); plane migration diagram of 3 fan bodies; (c) plane map of the 3 fan bodies.

The turbidite fan in the study area exhibits an obvious migration pattern. Early fan sedimentation occurred in the low-lying areas of the basin. With the increasing effect of infilling and compensation, the original paleogeomorphology was changed. Later, the fan would migrate to the side that had been transformed into a relatively lower-lying area. Due to differences in sediment supply and accommodation space, the size of the fan will undergo varying degrees of change during the migration process.

5.4. Sedimentary Model

Based on lithology, sedimentary structures, and facies analysis, this study analyzed the sedimentary characteristics of the turbidite fan system in the study area and summarized the sedimentary model of the fan system. The study area is located in the gentle slope zone of the Chezhen Depression, with the source mainly being the Wudi and Yihetuan Uplifts in the south. During the deposition of the Es3U, sediment from the uplifts was sequentially deposited as river and delta sediment along the gentle slope zone, and the turbidite fan system in the study area was deposited at the front end of the delta. After long-distance transportation, the sediment size on the gentle slope zone had become finer, resulting in the overall fine-grained composition of the turbidite fan system in the study area, with mainly siltstone forming the vertical facies sequence pattern of siltstone turbidite. The overall performance of the fan system is characterized by thin layers, a small scale, and fast facies changes (Figure 6).

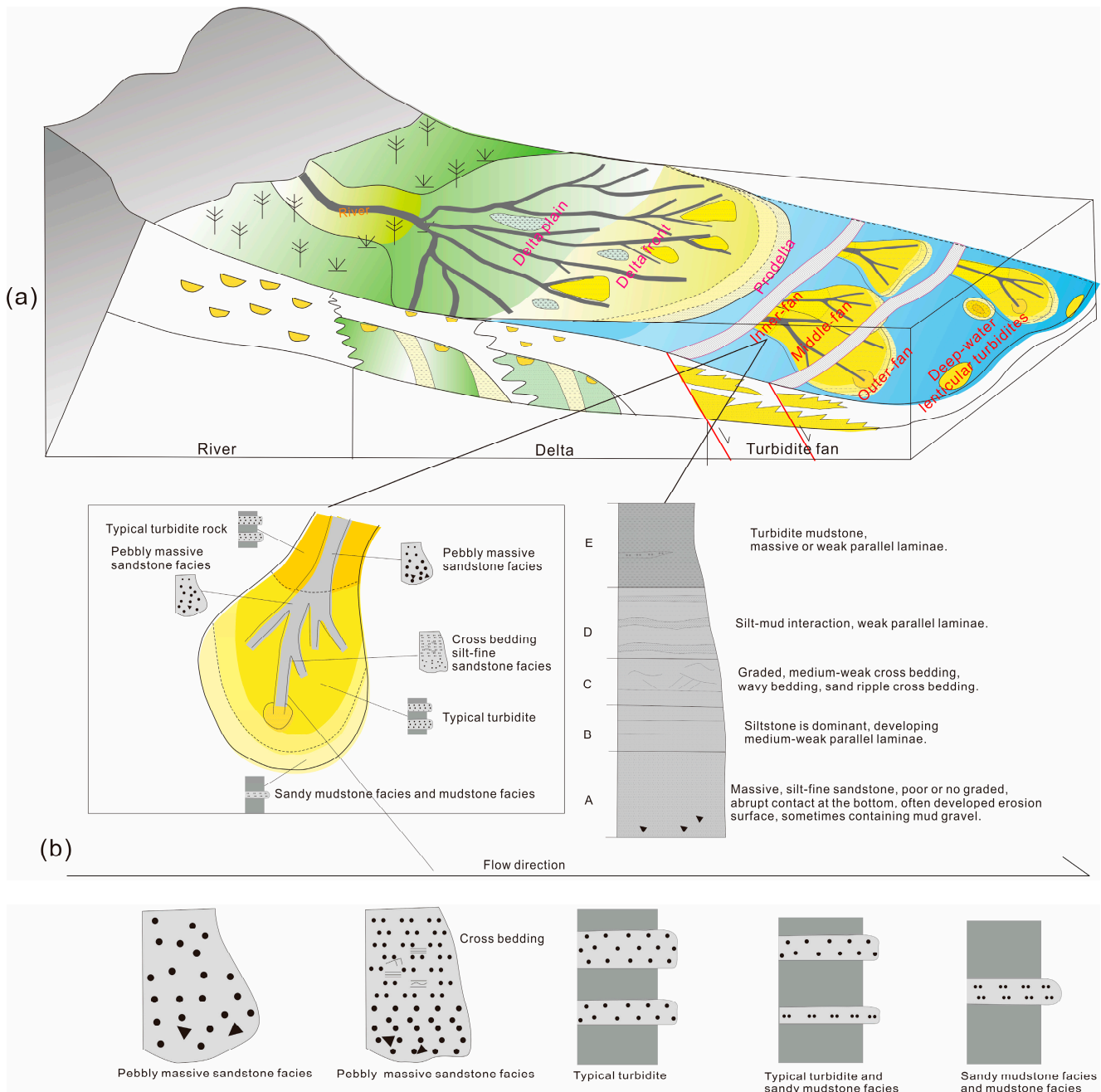


Figure 6. Sedimentary model of a turbidite fan in the study area. (a) The geological and environmental context in which a turbidite fan was formed. (b) Planar distribution and vertical sequence profile of a turbidite fan.

This model does not show typical Bouma sequences, and only incomplete Bouma sequences can be seen in sedimentary facies belts such as the mid-fan braid channel and the front edge of the fan. However, layer segments equivalent to Bouma sequences can be identified. A complete Bouma sequence segment includes a bottom graded layer (A segment), lower parallel lamination layer (B segment), flow ripple lamination layer (C segment), upper parallel lamination layer (D segment), and deep water mud shale layer (E segment) from the bottom up. In the siltstone turbidite facies sequence of the study area, because the sediment size is relatively fine, the A segment shows a massive sandstone facies (Sc) with mud gravel at the bottom, generally with poor or no grading. The point is that scour surfaces and mud gravel are often developed at the bottom. The

B segment is the lower parallel lamination layer, but parallel bedding is often not developed in the sedimentary sequence in the study area, and even if it is developed, it is similar to the massive sandstone facies with finer grains and basically no mud gravel. The typical feature of the C segment is flow ripple bedding, and a small amount of weak to moderate cross-bedding can be recognized in the study area, generally being a combination of ripple cross-bedding and sand wave cross-bedding, showing weak grading characteristics, but the C segment is not common in the study area. When the D segment is deposited, the water energy is obviously weak, and the lithology is fine, characterized by the interbedding of silt and mud, with weak parallel lamination commonly occurring, and sedimentary structures such as slides, load casts, and sand pillows develop, possessing the typical characteristics of turbidite rocks. The E segment is a shale section, with thin layers of silt and muddy silt developed, generally massive or with weak horizontal bedding (Figure 6).

6. Conclusions

- (1) The Chezhen Depression is a continental faulted basin with a gentle slope and a small far-source turbidite fan. Due to long-distance transportation, the grain size of the turbidite fan is fine, forming a vertical facies sequence pattern of siltstone turbidite. In the vertical direction, an incomplete Bouma sequence can be observed.
- (2) The turbidite deposits in the study area have characteristics such as a small scale, frequent migration and evolution, and a complex internal structure. Seven lithofacies could be identified within the study interval. Based on the combination of the lithofacies, a turbidite fan could be classified into seven micro-facies and three sub-facies. Among them, the braided channel micro-facies in the middle fan sub-facies is the most important sand body type.

Author Contributions: Conceptualization, J.L.; data curation, D.D.; methodology, J.L.; project administration, J.L.; resources, X.H.; supervision, J.L.; validation, X.H. and D.D.; writing—original draft, J.C.; writing—review and editing, J.C., X.H., D.D. and J.L. All authors have read and agreed to the published version of the manuscript.

Funding: This research has been supported by the National Natural Science Foundation of China (grant no. 42002169), the Seven-Year Oil and Gas Action Plan of CNOOC (grant no. CNOOC-KJ 135 ZDXM 39 SH01 & CNOOC-KJ 135 ZDXM 39 SH03), the Initial Fund for Young Scholars of Qingdao University of Science and Technology, and the Open Fund of State Key Laboratory of Oil and Gas Reservoir Geology and Exploitation (Chengdu University of Technology) (grant no. PLC20210113).

Data Availability Statement: Raw data reserved.

Conflicts of Interest: The authors declare no conflict of interest.

References

1. Bouma, A.H. *Sedimentology of Some Flysch Deposits: A Graphic Approach to Facies Interpretation*; Elsevier: Amsterdam, The Netherlands, 1962; Volume 168.
2. Bouma, A.H. Turbidites. In *Developments in Sedimentology*; Elsevier: Amsterdam, The Netherlands, 1964; Volume 3, pp. 247–256.
3. Bouma, A.H. Key controls on the characteristics of turbidite systems. *Geol. Soc. Lond. Spec. Publ.* **2004**, *222*, 9–22. [[CrossRef](#)]
4. Walker, R.G. The origin and significance of the internal sedimentary structures of turbidites. *Proc. Yorks. Geol. Soc.* **1965**, *35*, 1–32. [[CrossRef](#)]
5. Walker, R.G. Facies, facies models, and modern stratigraphic concepts. In *Facies Models: Response to Sea Level Change, GEO Text 1*; Walker, R.G., James, N.P., Eds.; Geological Association of Canada: St. John's, NL, Canada, 1992; pp. 1–14.
6. Shepard, F.P.; Marshall, N.F.; McLoughlin, P.A.; Sullivan, G.G. Currents in submarine canyons and other sea valleys. *AAPG Stud. Geol.* **1979**, *8*, 173.
7. Gervais, A.; Savoye, B.; Mulder, T.; Gonthier, E. Sandy modern turbidite lobes: A new insight from high resolution seismic data. *Mar. Pet. Geol.* **2006**, *23*, 485502. [[CrossRef](#)]
8. Stow, D.A.V.; Faugères, J.-C. Contourite facies and the facies model. In *Contourites*; Rebesco, M., Camerlenghi, A., Eds.; Elsevier: Amsterdam, The Netherlands, 2008; pp. 223–256.
9. Shanmugam, G.; Moiola, R.J. Eustatic control of turbidites and winnowed turbidites. *Geology* **1982**, *10*, 231–235. [[CrossRef](#)]
10. Shanmugam, G.; Moiola, R.J. Reinterpretation of depositional processes in a classic flysch sequence (Pennsylvanian Jackfork Group), Ouachita Mountains, Arkansas and Oklahoma. *AAPG Bull.* **1995**, *79*, 672–695.

11. Shanmugam, G.; Shrivastava, S.K.; Das, B. Sandy debrites and tidalites of Pliocene reservoir sands in upper-slope canyon environments, Offshore Krishna-Godavari Basin (India): Implications. *J. Sediment. Res.* **2009**, *79*, 736–756. [[CrossRef](#)]
12. Shanmugam, G. Modern internal waves and internal tides along oceanic pycnoclines: Challenges and implications for ancient deep-marine baroclinic sands. *AAPG Bull.* **2013**, *97*, 767–811. [[CrossRef](#)]
13. Pellegrini, C.; Maselli, V.; Trincardi, F. Pliocene–Quaternary contourite depositional system along the south-western Adriatic margin: Changes in sedimentary stacking pattern and associated bottom currents. *Geo-Mar. Lett.* **2016**, *36*, 67–79. [[CrossRef](#)]
14. Fonesu, M.; Palermo, D.; Galbiati, M.; Marchesini, M.; Bonamini, E.; Bendias, D. A new world-class deep-water play-type, deposited by the syndepositional interaction of turbidity flows and bottom currents: The giant Eocene coral field in northern Mozambique. *Mar. Pet. Geol.* **2020**, *111*, 179–201. [[CrossRef](#)]
15. Gauchery, T.; Rovere, M.; Pellegrini, C.; Asioli, A.; Tesi, T.; Cattaneo, A.; Trincardi, F. Post-LGM multi-proxy sedimentary record of bottom-current variability and downslope sedimentary processes in a contourite drift of the Gela Basin (Strait of Sicily). *Mar. Geol.* **2021**, *439*, 106564. [[CrossRef](#)]
16. Zhang, S.; Sui, F.; Wang, Y. Steep bank sedimentary model of the Lower Tertiary in Jiyang Depression. *Acta Sedimentol. Sin.* **2001**, *19*, 5.
17. Wang, B.Y.; Sui, F.G. Classification and distribution of gravelly rock bodies in steep slope zones of faulted and sagged lake basins in Jiyang Depression. *Spec. Oil Gas Reserv.* **2003**, *10*, 38–41.
18. Jiang, S.H.; Lin, H.M.; Wang, Y.S. Characteristics of oil and gas accumulation in the steep-slope sand-gravel fan: A case study of the Jiyang Depression. *Geophys. Prospect. Pet.* **2003**, *42*, 5.
19. Hou, G.Q. Sedimentary Characteristics and Distribution Evaluation of Turbidite Sandbodies in the Third and Fourth Members of Shahejie Formation in Niuzhuangwa Sag. Master's Thesis, Chengdu University of Technology, Chengdu, China, 2016.
20. Lao, H.; Wang, Y.; Shan, Y.; Hao, X.; Li, Q. Hydrocarbon downward accumulation from an upper oil source to the oil reservoir below in an extensional basin: A case study of Chezhen Depression in the Bohai Bay Basin. *Mar. Pet. Geol.* **2019**, *103*, 516–525. [[CrossRef](#)]
21. Wang, L.; Zhang, J.; Zhang, Y. Sedimentary environment of Shahejie Formation in Chezhen Sag, Bohai Bay Basin, China. *Arab. J. Geosci.* **2021**, *14*, 2159. [[CrossRef](#)]
22. Li, J.; Zhang, J.; Sun, S.; Zhang, K.; Du, D.; Sun, Z.; Wang, Y.; Liu, L.; Wang, G. Sedimentology and mechanism of a lacustrine syn-rift fan delta system: A case study of the Paleogene Gaobei Slope Belt, Bohai Bay Basin, China. *Mar. Pet. Geol.* **2018**, *98*, 477–490. [[CrossRef](#)]
23. Xian, B.Z.; Wu, C.X.; She, Y.Q. Paleogene fluid abnormal high pressure and its effect on deep clastic reservoirs in Chezhen Sag, Dongying Depression, Shandong. *J. Palaeogeogr.* **2011**, *3*, 309–316.
24. Zhu, X.M.; Zhao, D.N.; Jiang, S.X.; Ge, J.W.; Zhang, S.P.; Han, X.F.; Liu, X. Diagenetic Sequence of Low Porosity of Permeability Reservoirs from Nearshore Subaqueous Fan of Shahejie Formation in the Steep Slope Zone of Chezhen Depression, Bohai Bay Basin. *J. Earth Sci. Environ.* **2014**, *36*, 1–9.
25. Li, J.; Yan, K.; Ren, H.; Sun, Z. Detailed quantitative description of fluvial reservoirs: A case study of L6-3 layer of sandgroup 6 in the second member of Shahejie Formation, Shengtuo Oilfield, China. *Adv. Geo-Energy Res.* **2020**, *4*, 43–53. [[CrossRef](#)]
26. Li, J.; Sun, Z.; Ren, H.; Gong, L.; Li, T.; Du, D. Magnetic random walk algorithm and its application in the distributary channel system reservoir modeling. *J. Pet. Sci. Eng.* **2020**, *206*, 109062. [[CrossRef](#)]
27. Li, Z.; Schieber, J.; Pedersen, P.K. On the origin and significance of composite particles in mudstones: Examples from the Cenomanian Dunvegan Formation. *Sedimentology* **2021**, *68*, 737–754. [[CrossRef](#)]
28. Zhang, J.; He, S.; Wang, Y.; Wang, Y.; Hao, X.; Luo, S.; Li, P.; Dang, X.; Yang, R. Main mechanism for generating overpressure in the Paleogene source rock series of the Chezhen depression, Bohai Bay Basin, China. *J. Earth Sci.* **2019**, *30*, 775–787. [[CrossRef](#)]
29. Wang, Y.; Lin, C. Discovery of the gravity gliding tectonic of Shanwang Formation, Shanwang Basin. *Northwest Geol.* **2008**, *41*, 5.
30. Stow, D.A.V. Deep-sea processes of sediment transport and deposition. In *Sediment Transport and Depositional Processes*; Pye, K., Ed.; Blackwell Scientific Publications: Hoboken, NJ, USA, 1994; pp. 257–293.
31. Kuehl, S.A.; DeMaster, D.J.; Nittrouer, C.A. Nature of sediment accumulation on the Amazon continental shelf. *Cont. Shelf Res.* **1986**, *6*, 209–225. [[CrossRef](#)]
32. Gauchery, T.; Rovere, M.; Pellegrini, C.; Cattaneo, A.; Campiani, E.; Trincardi, F. Factors controlling margin instability during the plio-quaternary in the Gela Basin (Strait of Sicily, Mediterranean Sea). *Mar. Pet. Geol.* **2021**, *123*, 104767. [[CrossRef](#)]
33. Amorosi, A.; Sammartino, I.; Dinelli, E.; Campo, B.; Guercia, T.; Trincardi, F.; Pellegrini, C. Provenance and sediment dispersal in the Po-Adriatic source-to-sink system unraveled by bulk-sediment geochemistry and its linkage to catchment geology. *Earth-Sci. Rev.* **2022**, *234*, 104202. [[CrossRef](#)]
34. Miramontes, E.; Pellegrini, C.; Casalbore, D.; Dupré, S. Active geological processes in the Mediterranean Sea. In *Oceanography of the Mediterranean Sea*; Elsevier: Amsterdam, The Netherlands, 2023; pp. 453–499.
35. Schieber, J. Mud re-distribution in epicontinental basins—Exploring likely processes. *Mar. Pet. Geol.* **2016**, *71*, 119–133. [[CrossRef](#)]
36. Smith, L.B.; Schieber, J.; Wilson, R.D. Shallow-water onlap model for the deposition of Devonian black shales in New York, USA. *Geology* **2019**, *47*, 279–283. [[CrossRef](#)]
37. Pellegrini, C.; Tesi, T.; Schieber, J.; Bohacs, K.M.; Rovere, M.; Asioli, A.; Nogarotto, A.; Trincardi, F. Fate of terrigenous organic carbon in muddy clinothems on continental shelves revealed by stratal geometries: Insight from the Adriatic sedimentary archive. *Glob. Planet. Chang.* **2021**, *203*, 103539. [[CrossRef](#)]

38. Beaubouef, R.T.; Rossen, C.; Zelt, F.; Sullivan, M.D.; Mohrig, D.; Jennette, D.C. Deep-Water Sandstones, Brushy Canyon formation West Texas. In Proceedings of the Field Guide for AAPG Hedberg Field Research Conference, West, TX, USA, 15–20 April 1999; AAPG Continuing Education Course Note Series #40; American Association of Petroleum Geologists: Tulsa, OK, USA, 1999; 48p.
39. Posamentier, H.W.; Kolla, V. Seismic Geomorphology and stratigraphy of depositional elements in Deep-Water Settings. *J. Sediment. Res.* **2003**, *73*, 367–388. [[CrossRef](#)]
40. Gamberi, F.; Pellegrini, C.; Dalla Valle, G.; Scarponi, D.; Bohacs, K.; Trincardi, F. Compound and hybrid clinothems of the last lowstand Mid-Adriatic Deep: Processes, depositional environments, controls and implications for stratigraphic analysis of prograding systems. *Basin Res.* **2020**, *32*, 363–377. [[CrossRef](#)]
41. Patruno, S.; Scisciani, V.; Helland-Hansen, W.; D’Intino, N.; Reid, W.; Pellegrini, C. Upslope-climbing shelf-edge clinoforms and the stepwise evolution of the northern European glaciation (lower Pleistocene Eridanos Delta system, UK North Sea): When sediment supply overwhelms accommodation. *Basin Res.* **2020**, *32*, 224–239. [[CrossRef](#)]
42. Pellegrini, C.; Patruno, S.; Helland-Hansen, W.; Steel, R.J.; Trincardi, F. Clinoforms and clinothems: Fundamental elements of basin infill. *Basin Res.* **2020**, *32*, 187–205. [[CrossRef](#)]
43. Allen, J.R.L. Studies in fluvial sedimentation: Bars, bar-complexes and sandstone sheets (low-sinuosity braided streams) in the Brownstones (L. Devonian), Welsh Borders. *Sediment. Geol.* **1983**, *33*, 237–293. [[CrossRef](#)]
44. Gardner, M.H.; Borer, J.M. Submarine Channel Architecture Along a Slope to basin Profile, Brushy Canyon formation, West Texas. In *Fine-Grained Turbidite Systems*; Bouma, A.H., Stone, C.G., Eds.; AAPG Memoir 72, SEPM Special Publication No. 68; American Association of Petroleum Geologists: Tulsa, OK, USA, 2000; pp. 195–214.
45. Kane, I.A.; Hodgson, D.M. Sedimentological criteria to differentiate submarine channel levee subenvironments: Exhumed examples from the Rosario Fm. (Upper Cretaceous) of Baja California, Mexico, and the Fort Brown Fm. (Permian), Karoo Basin, S. Africa. *Mar. Pet. Geol.* **2011**, *28*, 807–823. [[CrossRef](#)]

Disclaimer/Publisher’s Note: The statements, opinions and data contained in all publications are solely those of the individual author(s) and contributor(s) and not of MDPI and/or the editor(s). MDPI and/or the editor(s) disclaim responsibility for any injury to people or property resulting from any ideas, methods, instructions or products referred to in the content.